Specific Deletion of CASK in Pancreatic β-Cells Affects Glucose Homeostasis and Improves Insulin Sensitivity in Obese Mice by Reducing Hyperinsulinemia

Xingjing Liu,[1] Peng Sun,[2] Qingzhao Yuan,[1] Jinyang Xie,[1] Ting Xiao,[1] Kai Zhang,[1] Xiu Chen,[1] Yao Wang,[1] Li Yuan,[2] and Xiao Han[2,3]

Diabetes 2022;71:104–115 | https://doi.org/10.2337/db20-1208

ISLET STUDIES

Calcium/calmodulin-dependent serine protein kinase (CASK) is involved in the secretion of insulin vesicles in pancreatic β-cells. The current study revealed a new in vivo role of CASK in glucose homeostasis during the progression of type 2 diabetes mellitus (T2DM). A Cre-loxP system was used to specifically delete the *Cask* gene in mouse β-cells (βCASKKO), and glucose metabolism was evaluated in βCASKKO mice fed a normal chow diet (ND) or a high-fat diet (HFD). ND-fed mice exhibited impaired insulin secretion in response to glucose stimulation. Transmission electron microscopy showed significantly reduced numbers of insulin granules at or near the cell membrane in the islets of βCASKKO mice. By contrast, HFD-fed βCASKKO mice showed reduced blood glucose and a partial relief of hyperinsulinemia and insulin resistance when compared with HFD-fed wild-type mice. The IRS1/PI3K/AKT signaling pathway was upregulated in the adipose tissue of HFD-fed βCASKKO mice. These results indicated that knockout of the *Cask* gene in β-cells had a diverse effect on glucose homeostasis; it reduced insulin secretion in ND-fed mice but improved insulin sensitivity in HFD-fed mice. Therefore, CASK appears to function in insulin secretion and contributes to hyperinsulinemia and insulin resistance during the development of obesity-related T2DM.

Pancreatic β-cells regulate glucose homeostasis by secreting insulin (1). When stimulated by glucose, pancreatic β-cells secrete insulin in a biphasic pattern (2). Subsequent insulin signaling, triggered by the interaction between insulin and the insulin receptor, in turn reduces glucose levels by suppressing hepatic gluconeogenesis and promoting glucose uptake in skeletal muscle and fat (3). However, in obesity and type 2 diabetes mellitus (T2DM), excessive intracellular lipid accumulation in the liver, adipose tissue, and skeletal muscle impairs insulin signaling, promotes systemic insulin resistance, and causes compensatory increase of serum insulin level (4). Long-term hyperinsulinemia aggravates the dysfunction of islet β-cells and leads to insulin resistance and failure to control glycemia (5). Therefore, further exploration of the mechanism of insulin secretion and the development of hyperinsulinemia is critical for T2DM treatment.

We previously reported that islet and β-cell lines highly express calcium/calmodulin-dependent serine protein kinase (CASK), a member of the membrane-associated guanylate kinase (MAGUK) protein family (6). CASK forms complexes with different binding partners and exhibits various functions (7,8), such as regulating neurotransmitter release by binding to different proteins. In pancreatic β-cells, our previous studies have demonstrated that CASK participates in insulin granule exocytosis in rat insulinoma INS-1 cells (9). Meanwhile, *Cask* knockdown in INS-1 cells reduces insulin release, possibly through effects on the anchoring process of insulin vesicles onto the β-cell membrane (10). Exendin-4–enhanced insulin release

[1]Department of Endocrinology, Zhongda Hospital, and Institute of Diabetes, Medical School, Southeast University, Nanjing, China

[2]Key Laboratory of Human Functional Genomics of Jiangsu Province, Department of Biochemistry and Molecular Biology, Nanjing Medical University, Nanjing, China

[3]State Key Laboratory of Pharmaceutical Biotechnology, Nanjing University, Nanjing, China

Corresponding authors: Yao Wang, 101007985@seu.edu.cn; Li Yuan, yuanli@njmu.edu.cn; and Xiao Han, hanxiao@njmu.edu.cn

Received 29 November 2020 and accepted 11 October 2021

This article contains supplementary material online at https://doi.org/10.2337/figshare.16797871.

X.L. and P.S. contributed equally to this article.

is also reduced in *Cask* knockdown INS-1 cells (11). More importantly, we have revealed that CASK is also involved in glucotoxicity- (12), palmitate- (10), or inflammatory cytokine–induced (13) impairment in pancreatic β-cells (12). These in vitro results reveal that CASK not only plays a crucial role in the physiological insulin secretion of islet β-cells, but also possibly contributes to β-cell injury during the development of T2DM. However, the exact in vivo role of CASK in insulin secretion and glucose homeostasis during the development of T2DM has not been elucidated.

Previous studies have shown that systemic *Cask* knockout mice were characterized by partially penetrating cleft palate syndrome and increased apoptosis of thalamus cells, and these mice died soon after birth (14,15). In the current study, we used a conditional knockout strategy in mice to delete *Cask* expression specifically in β-cells, and we examined the effect of this CASK knockdown on insulin secretion and glucose homeostasis. Moreover, whether CASK deletion in β-cells affects the development of hyperinsulinemia and insulin resistance was also investigated in mice fed a high-fat diet (HFD).

RESEARCH DESIGN AND METHODS

Mice

C57BL/6J mice and MIP-CreERT mice were obtained from the Model Animal Research Center of Nanjing University (Nanjing, China). $CASK^{fl/fl}$ mice, in which exon 6 of the *Cask* gene is flanked by two loxP sites, were generated by Cyagen Biosciences (Suzhou, China). The deletion of exon 6 of the *Cask* gene caused a frameshift mutation and loss of function. The designed mouse genomic fragments were 5′homologous sequence loxP conditional knockout region-positive screening marker gene Neo-loxP 3′homologous sequence-negative screening marker gene DTA; this system was assembled into a vector. The purified targeting vector was delivered to embryonic stem cells (C57BL/6J) by electroporation, followed by bidirectional (positive and negative) drug identification screening. The positive clones were analyzed by Southern blotting to further confirm the homologous recombination. The targeted embryonic stem cells were microinjected into C57BL/6J blastocysts, which were then implanted into pseudopregnant mice to generate chimeric mice. The genotype of the mice was analyzed by PCR using mouse tail genomic DNA. The primers for genotyping of the $CASK^{fl/fl}$ allele were as follows: F1, GCTAAAGTCATCAGCCTATGTG; R1, GCAGTACAGAATGGAGAACTGCAA. All animals were housed at 22 ± 1°C, with relative humidity of 50 ± 1% and a 12/12-h light/dark cycle. The 24-h food intake and feces excretion of individual mice in metabolic cages were recorded. All the animal studies (including mouse euthanasia) were conducted in compliance with the regulations and guidelines of Nanjing Medical University institutional animal care (Nanjing, China) according to Association for Assessment and Accreditation of Laboratory Animal Care and Institutional Animal Care and Use Committee guidelines (1702004).

$CASK^{fl/fl}$ mice were crossed with MIP-CreERT mice (expressing Cre recombinase under the control of the mouse insulin 1 promoter (16)) to create β-cell–specific CASK knockout mice (MIP-CreERT; $CASK^{fl/fl}$; βCASKKO). The βCASKKO mice were born at the expected Mendelian ratios. All offspring were identified by PCR (Supplementary Fig. 1*A*). To avoid interference of the Cre transgene and tamoxifen in the mouse metabolic phenotype (17), we used wild-type (WT), Cre, and Flox mice as littermate controls. Four-week-old mice were intraperitoneally injected with 150 mg/kg tamoxifen (Sigma-Aldrich, St Louis, MO) for 7 days to induce recombination of floxed alleles. To further elucidate the role of CASK in obesity-associated metabolic dysfunction, we assessed the metabolic phenotypes in mice fed an HFD for either 8 or 16 weeks. The animals were fed a normal chow diet (ND) or HFD (60% fat, 20% protein, and 20% carbohydrate) (catalog no. D12492; Research Diets, New Brunswick, NJ).

Western Blotting

Tissue samples or isolated islets were lysed in protein lysis buffer for the subsequent Western blotting analysis as previously described (18). The antibodies used are listed in Supplementary Table 2. Densitometry analyses were quantified using ImageJ software. Specifically, to investigate the effect of β-cell–specific knockout of CASK on insulin sensitivity in mice fed an HFD for 16 weeks, the mice were injected intraperitoneally with insulin (1 unit/kg body weight) after a 4-h fast. After 15 min, liver, muscle, and adipose tissue samples from mice were removed and lysed, and the phosphorylation of insulin signaling–mediated proteins was determined by Western blotting analysis.

Real-Time Quantitative PCR Analysis

Total RNA was extracted using an RNA extraction kit (Invitrogen) and reverse transcribed to cDNA using the PrimeScript RT Reagent Kit (Takara Bio, Tokyo, Japan). Quantitative PCR (qPCR) was performed using the SYBR Premix Ex TaqTMII Kit (Takara Bio) on the Roche LightCycler 480 System (Roche, Basel, Switzerland). Primer sequences are listed in the Supplementary Materials.

Histopathological Analysis

Mouse tissues were fixed and embedded in paraffin for morphological staining. Primary antibodies for CASK (1:200) (Santa Cruz Biotechnology), insulin (1:500) (Wuhan Servicebio Technology, Wuhan, China), and glucagon (1:500) (Wuhan Servicebio Technology) were diluted in blocking buffer. For immunofluorescence, nuclei were counterstained with Hoechst 33342 (Sigma-Aldrich). Rhodamine-labeled anti-rabbit IgG (1:40) (Chemicon International, Temecula, CA) was used as the secondary antibody. The stained tissue sections were observed by

confocal laser scanning microscopy (LSM710; Carl Zeiss, Oberkochen, Germany). For immunohistochemical staining, the Max-Vision HRP-Polymer Immunohistochemical Kit (Fuzhou Maixin Biotech, Fuzhou, China) was used; after primary antibody incubation, the sections were observed under an optical microscope (DP70; Olympus). The calculation of β-cell mass was performed as previously described (19).

Blood Glucose and Plasma Insulin Measurements

Fasting blood glucose and insulin were measured after a 12-h fast. Blood glucose levels in samples collected from the tail vein were measured with a glucometer monitor (Bayer). Plasma insulin levels were measured using a commercial ELISA kit (Mercodia).

Glucose Tolerance and Insulin Tolerance Tests

The intraperitoneal injection of glucose tolerance test was performed after overnight fasting. The mice were injected with glucose (1.5 g/kg body weight), and the blood levels were measured at specific time points with a glucometer monitor (Bayer) (a Roche ACCU-CHEK glucose meter was used for HFD-fed mice). The area under the curve (AUC) was calculated based on the trapezoidal rule (0–120 min). To calculate the incremental AUC, the intraperitoneal injection of glucose tolerance test curve was normalized to the baseline blood glucose of each group.

The intraperitoneal injection of insulin tolerance test (IPITT) was performed in 4-h fasted mice by intraperitoneal injection of 1 unit/kg insulin. Blood glucose concentrations were measured from the tail vein using the glucometer monitor. For the statistical analysis of the IPITT curve, the rate of decline in the glucose level between 0 and 15 min was calculated using the log-transformed absolute glucose values (20).

Glucose-Stimulated Insulin Secretion Tests

For the in vivo glucose-stimulated insulin secretion (GSIS) test, mice were fasted and intraperitoneally injected with a glucose solution (1.5 g/kg body weight). The AUC was normalized to the baseline and calculated based on the trapezoidal rule (0–60 min). Venous blood samples were collected from the tail vein at specific time points, serum was obtained by centrifugation, and the insulin levels were measured using the ELISA kit.

For the in vitro static GSIS test, islets were isolated by collagenase digestion and Ficoll density gradient centrifugation and then cultured in RPMI 1640 medium with 10% FBS and 1% penicillin-streptomycin as previously described (21). The insulin content in GSIS samples was determined by radioimmunoassay (Beijing Northern Institute of Biotechnology Co., Ltd).

Hyperinsulinemic-Euglycemic Clamp Assays

Mice were anesthetized with isofluorane after a 4-h fast. The right internal jugular vein was cannulated with a catheter under aseptic surgical conditions as described previously (22). The catheter was then passed through a subcutaneous tunnel to the back of the neck. Each mouse was housed individually in a cage following the surgical procedure, and hyperinsulinemic-euglycemic clamp experiments were performed after allowing the animals to recover for 5–6 days. The mice were fasted for 4 h before the clamp experiments, and blood glucose was measured from the tail vein. The clamp was initiated at $t = 0$ min with a continuous infusion of insulin (Humulin; 4 mU/kg/min) and a variable glucose infusion rate (GIR) to induce hyperinsulinemia. The initial glucose infusion speed was 30 mg/kg/min (GIR), and blood glucose was measured every 10 min to maintain the target glycemic levels (∼15 mg/L) from $t = 0$ to 120 min. Before and 120 min after glucose perfusion, the basal and clamped serum insulin levels were measured. The liver, skeletal muscle, and adipose tissue were harvested at the end of the clamp experiment to measure the degree of AKT phosphorylation as an insulin sensitivity assessment.

Islet Perfusion

Islets were isolated and cultured overnight. A total of 200 islets were picked under a light microscope and placed in a perfusion chamber for perfusion with Krebs bicarbonate buffer for 30 min to reach the baseline hormone secretion values. The perfusion fluid was then collected every minute, and the islets were stimulated with 20 mmol/L high glucose or 50 mmol/L high potassium after 5 min. The insulin content in the perfusion fluid samples was determined by radioimmunoassay (Beijing Northern Institute of Biotechnology Co., Ltd).

Transmission Electron Microscopy

Islets were fixed overnight at 4°C in 2.5% glutaraldehyde in 0.1 mol/L sodium cacodylate buffer (pH 7.4) and then postfixed with 1% osmium tetroxide for 1 h. Following serial alcohol dehydration (50, 75, 95, and 100%), the samples were embedded in epon, cut into 12.70-nm sections, and stained with uranyl acetate for examination with a JEOL 1230 transmission electron microscope. Dense-core granules, empty granules, granule diameters, and distances from the cellular membrane were determined by manual counting and quantified using ImageJ software as previously described (23).

Statistical Analysis

All data were expressed as mean ± SD. Numerical differences between the two groups were assessed using the Student t test. One-way ANOVA with the Dunnett test was performed for data consisting of three groups, and two-way ANOVA was used for multiple comparisons. All data analyses were carried out using Prism 8 (GraphPad Software, San Diego, CA). $P < 0.05$ was considered statistically significant.

Data and Resource Availability

The data sets generated and analyzed during the current study are available from the corresponding author.

RESULTS

Pancreatic β-Cell–Specific Knockout of CASK in Mice

We assessed the effects of CASK on glucose metabolism and circumvented embryonic lethality by crossing MIP-CreERT male mice with loxP-flanked CASK$^{fl/fl}$ females (Fig. 1*A*). The mRNA quantification showed that the *Cask* level was 60% lower in islets from βCASKKO than from WT mice (Fig. 1*B*). Western blotting and immunofluorescence staining further confirmed a significant reduction in CASK expression in β-cells but no distinct changes in other tissues (Fig. 1*C–D*). No differences were detected between βCASKKO mice and littermate controls (WT, MIP-CreERT transgenic, and Flox mice) in body weight, food intake, body size, or overall behavior when fed the ND (Fig. 1*E*).

βCASKKO Mice Showed Impaired Insulin Secretion Under ND

We evaluated the difference in fasting blood glucose and postprandial blood glucose between the βCASKKO mice and the control (WT, MIP-CreERT transgenic, and Flox mice) littermates at ages 8, 12, and 16 weeks. No significant differences were noted in the fasting and postprandial blood glucose levels between the groups (Fig. 2*A–B*).

At age 16 weeks, higher blood glucose levels in the βCASKKO mice were found at 15 min after glucose injection than in other groups (Fig. 2*C*); nevertheless, the AUC did not show statistical difference. In IPITT, no significant difference was detected among the groups in blood glucose levels or the rate of decline in glucose between 0 and 15 min following intraperitoneal insulin injection (Fig. 2D). Hematoxylin-eosin staining of insulin target tissue sections showed normal morphology for the liver, muscle, and epididymal adipose tissues (Supplementary Fig. 2*A–C*) and similar AKT phosphorylation levels (Supplementary Fig. 2*D–F*) in these tissues in both the WT and βCASKKO mice.

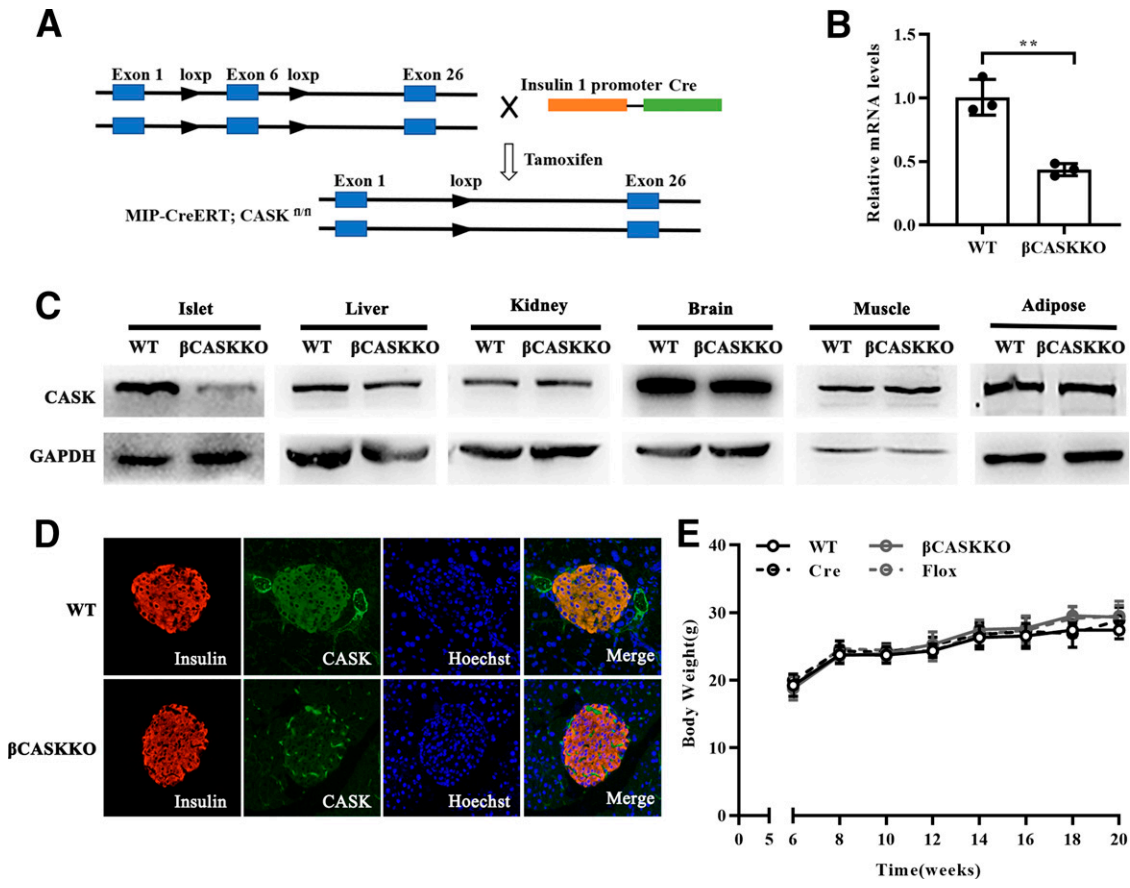

Figure 1—Selective knockout of the *Cask* gene in pancreatic β-cells. *A*: Schematic of the insertion of the loxp site on both sides of exon 6 of the *Cask* gene. All mice were administered tamoxifen at 4 weeks of age. *B*: The *Cask* mRNA level from WT and βCASKKO islets was measured by qPCR and normalized to that of *GAPDH* (n = 3 mice per group). *C*: Western blotting was performed for CASK and GAPDH from WT and βCASKKO islets (n = 3 mice per group). *D*: Immunofluorescence staining (staining with insulin [red] and CASK [green] antibodies) was performed for WT and βCASKKO mice. *E*: Body growth curves of WT, βCASKKO, Cre, and Flox mice at 6–20 weeks of age and fed an ND (n = 6). $^{**}P < 0.01$.

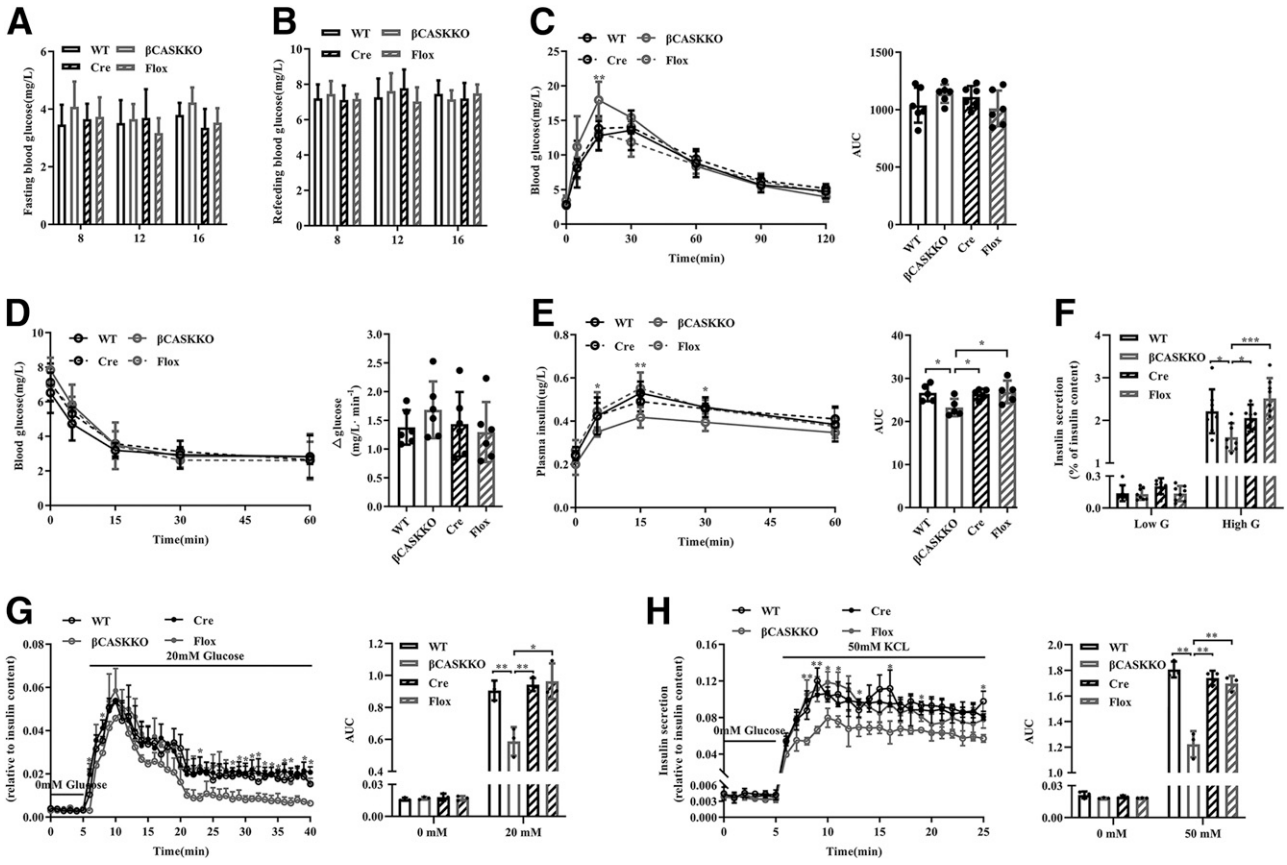

Figure 2—βCASKKO mice had increased blood glucose after glucose challenge and decreased insulin secretion. *A–B*: Fasting (*A*) and postprandial (*B*) blood glucose levels of mice (n = 6). *C*: Intraperitoneal glucose tolerance test assays were performed in 16-week-old mice. The AUC is shown on the right (n = 6). *D*: IPITT assays were performed in the mice after a 4-h fast. The rate of decline in glucose between 0 and 15 min is shown on the right (n = 6). *E*: Plasma insulin levels in overnight-fasted (12 h) mice were measured at the indicated time points after an intraperitoneal injection of 1.5 g/kg glucose (n = 5). AUC is shown on the right. *F*: Isolated mouse islets were cultured and incubated in either 3.3 or 16.7 mmol/L glucose for 1 h. Insulin release in response to glucose stimulation was calculated as a percentage of insulin content in the corresponding islets (n = 8). *G–H*: Islet perfusion assays were performed in mouse islets stimulated with 0 mmol/L glucose for 6 min, followed by 20 mmol/L glucose for 35 min (*G*) or 50 mmol/L potassium chloride for 20 min (*H*) (n = 4 mice per group). AUC is shown on the right. The experiments were repeated three times. *$P < 0.05$, ** $P < 0.01$, ***$P < 0.001$.

GSIS tests performed on 16-week-old mice revealed lower insulin-releasing levels in βCASKKO mice in comparison with other groups (Fig. 2*E*). In line with these in vivo data, GSIS tests performed on pancreatic islets isolated from the mice revealed lower insulin secretion by βCASKKO islets than by other groups (Fig. 2*F*).

The islet perfusion assays of dynamic insulin secretion revealed a typical biphasic response of insulin secretion in the pancreatic islets from both mouse groups following high glucose stimulation. Noticeably, insulin secretion was significantly inhibited in the βCASKKO islets (Fig. 2*G*). High potassium-stimulated insulin secretion was also decreased in βCASKKO islets compared with those of other groups (Fig. 2*H*).

Insulin Vesicle Transport to Cell Membrane Was Attenuated in Islet β-Cells From βCASKKO Mice

The MIP-CreERT transgenic mice and Flox mice did not show any abnormalities in glucose metabolism; therefore, we used WT mice as the controls for subsequent experiments. qPCR performed to elucidate the mechanism of insulin secretion dysfunction in βCASKKO mice revealed that CASK knockout did not affect the expression of genes involving insulin synthesis or exocytosis (Fig. 3*A*). Histological analysis did not reveal any difference in islet shape or size between βCASKKO and WT mice (Fig. 3*B*). Islet-specific staining showed similar cell arrangements and compositions in βCASKKO and WT mice (Fig. 3*C*).

Electron microscopy examination further confirmed no significant alterations in morphology, size, or number of insulin dense-core vesicles in βCASKKO versus WT islets (Fig. 3*D–F*). However, the number of vesicles at or near the cell membrane was significantly lower in the βCASKKO islets (Fig. 3*D*,*G*).

Reduced Hyperglycemia, Hyperinsulinemia, and Insulin Resistance Were Observed in βCASKKO Mice Fed HFD for 16 Weeks

We further assessed the role of CASK in obesity-associated metabolic dysfunction by examining the metabolic

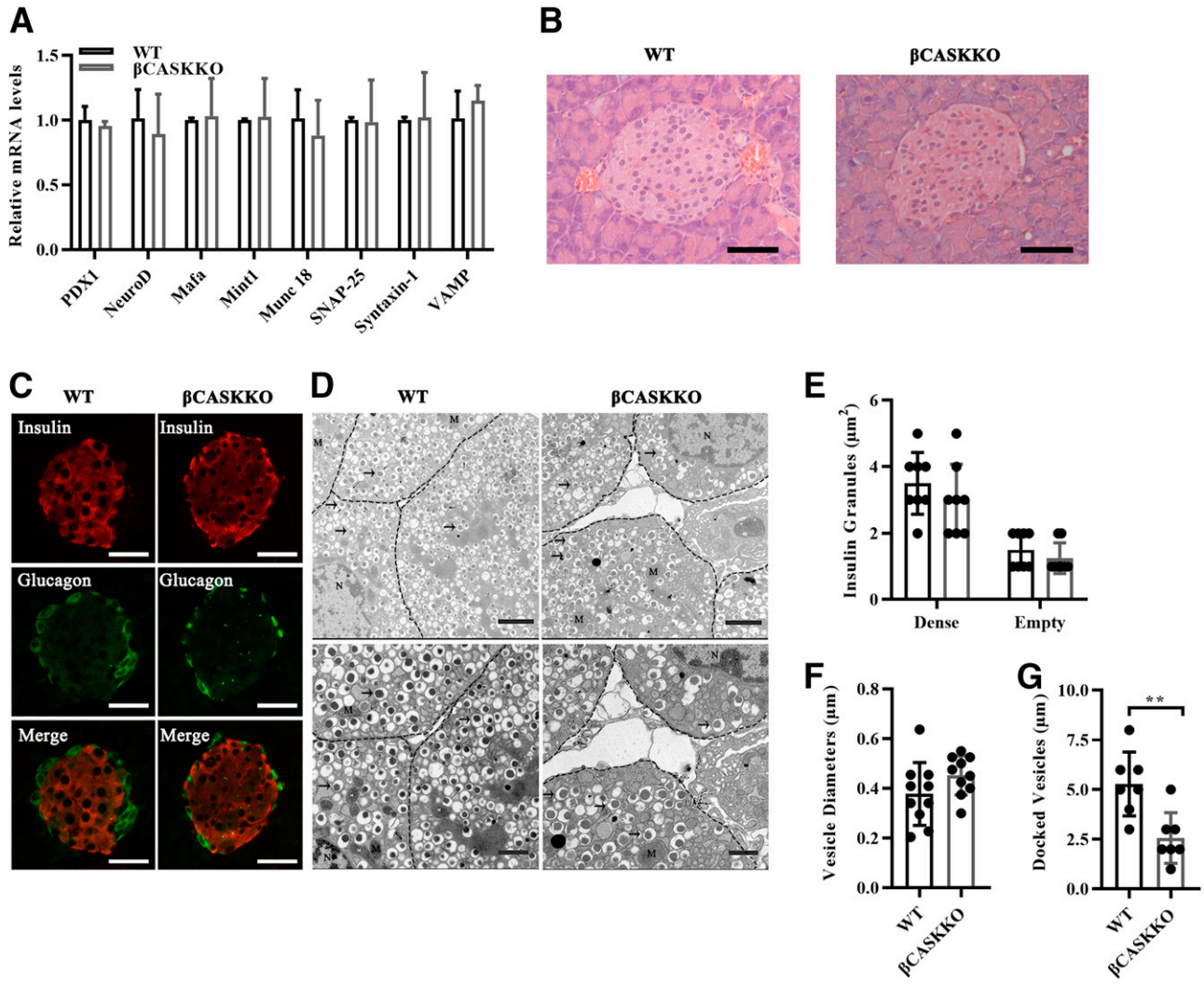

Figure 3—βCASKKO mice do not show islet developmental abnormalities. *A*: Quantitative Real-time qPCR to assess the mRNA levels in mouse islets. mRNA levels were normalized to *GAPDH* ($n = 4$ mice per group). *B*: Representative hematoxylin-eosin staining of pancreatic sections of WT and βCASKKO mice (scale bars 100 μm). *C*: Immunofluorescence histochemical analysis of pancreas sections of WT and βCASKKO mice (staining with insulin [red] and glucagon [green] antibodies). *D*: Transmission electron microscopy analysis of mouse islet (scale bars 2 [upper] and 1 μm [lower]). The gray dashed line outlines the plasma membrane; black arrowheads denote insulin granules. *E*: The number of mature (dense-core) and empty insulin granules per μm^2. *F*: The diameters of insulin vesicles were calculated based on the vesicle area. *G*: The number of insulin vesicles docked to the plasma membrane in WT and βCASKKO mice. A docked vesicle was defined as a vesicle with a distance from its center to the plasma membrane within 20 nm. The numbers were normalized per 1 μm of plasma membrane. $^{**}P < 0.01$. M, mitochondria; N, nucleus.

phenotypes of 10-week-old WT and βCASKKO mice fed an HFD for either 8 or 16 weeks. No differences were observed in food intake or feces excretion between the βCASKKO and WT mice during the 12-h day/night cycle (Supplementary Fig. 3*A–B*). Fig. 4*A* shows that mice fed the HFD for 16 weeks had significantly increased body weight in comparison with ND-fed mice; as in ND-fed mice, βCASKKO did not alter the body weight of HFD-fed animals. Immunoblotting and qPCR analysis confirmed CASK expression was higher in the islets from HFD-fed WT mice than those from ND-fed WT mice (Fig. 4*B–C*).

Strikingly, after consuming the HFD for 16 weeks, HFD-fed βCASKKO mice showed reduced fasting blood glucose (Fig. 4*D*) but not refeeding blood glucose (Fig. 4*E*) compared with HFD-fed WT mice. Meanwhile, plasma insulin levels were also lower in HFD-fed βCASKKO mice (Fig. 4*F*) than in HFD-fed WT mice. Unlike the results in ND-fed mice, the HFD-fed βCASKKO mice showed a significant improvement in glucose tolerance (Fig. 4*G*) and insulin sensitivity (Fig. 4*H*). In response to glucose challenge, the HFD-fed βCASKKO mice secreted lower levels of insulin compared with HFD-fed WT mice (Fig. 4*I*). In vitro GSIS tests performed in islets from HFD-fed mice also showed lower insulin secretion by islets from HFD-fed βCASKKO mice than by those from HFD-fed WT mice (Fig. 4*J*). Insulin-stained sections (Fig. 4*K*) and

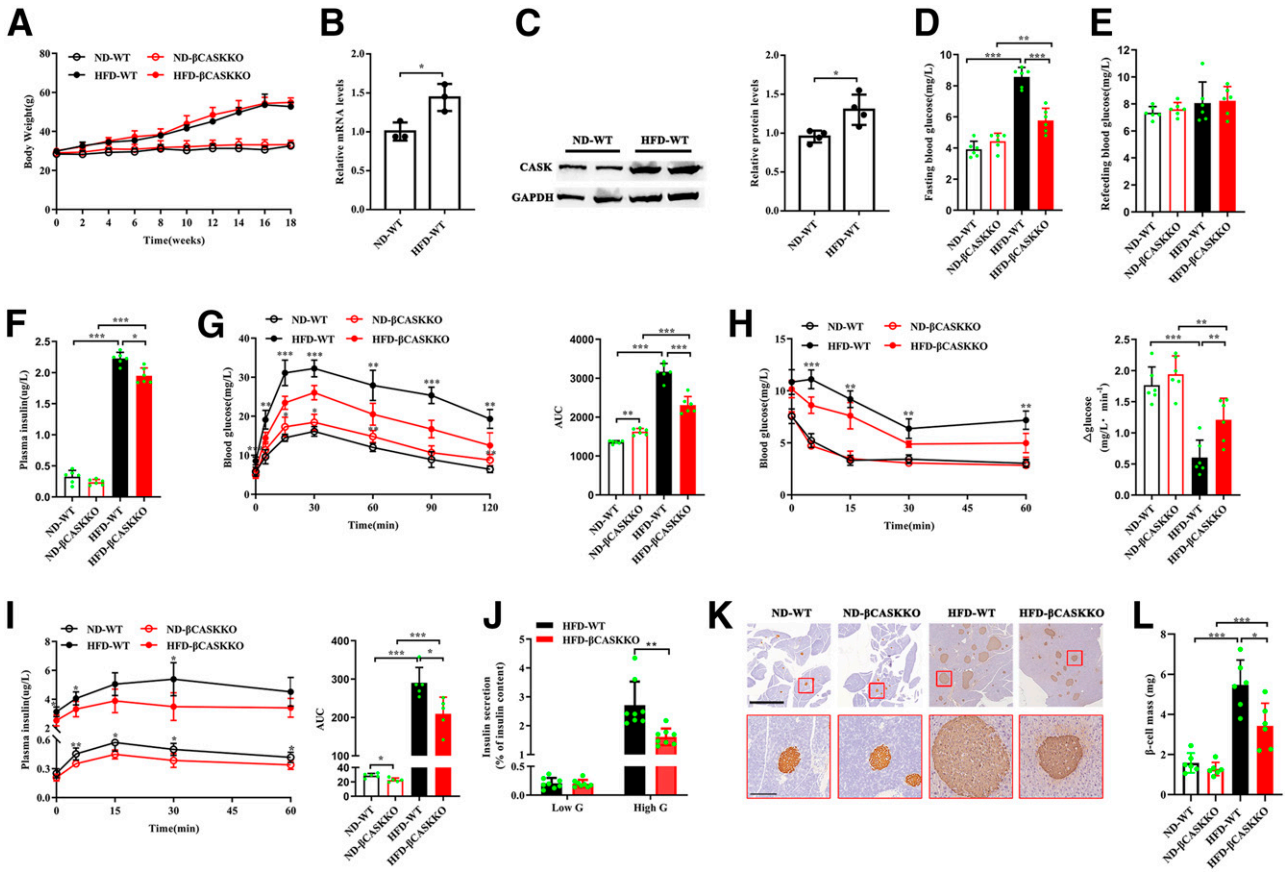

Figure 4—HFD for 16 weeks improved abnormal glucose metabolism in HFD-fed βCASKKO mice. *A*: Body weight of WT and βCASKKO mice fed an ND and HFD (n = 5–7). *B*: The *Cask* mRNA level from WT and βCASKKO islets was measured by qPCR and normalized to that of *GAPDH* (n = 3 mice/group). *C*: Western blot and densitometry data analysis of CASK and GAPDH in islets from ND-fed WT and HFD-fed WT mice (n = 4 mice per group). *D–F*: Fasting (*D*) and postprandial (*E*) blood glucose levels and fasting serum insulin level (*F*) of WT and βCASKKO mice after HFD and ND feeding at the week indicated (n = 6). *G–H*: Glucose tolerance test (*G*) and insulin tolerance test (*H*) assays were conducted in mice after 16 weeks of HFD or ND feeding (n = 6). *P* values for WT versus βCASKKO. The AUC or rate of decline in glucose between 0 and 15 min is shown on the right side of the corresponding curve. *I*: GSIS assays were performed in mice (n = 5). *P* values for WT versus βCASKKO. The AUC is shown on the right. *J*: Pancreatic islets of HFD-fed mice were isolated to perform in vitro GSIS assays. Insulin release in response to glucose stimulation was calculated as a percentage of insulin content in the corresponding islets (n = 8). *K*: Immunohistochemistry of the pancreatic sections for insulin (brown, bottom row) are shown. *L*: Average β-cell mass (n = 8). $*P < 0.05$, $**P < 0.01$, $***P < 0.001$.

quantitative β-cell mass (Fig. 4*L*) indicated the compensatory increase of islet β-cell mass in HFD-fed βCASKKO mice was lower compared with that in HFD-fed WT mice.

The hyperinsulinemic-euglycemic clamp assays were performed after 16-week feeding of HFD. Figure 5*A* suggests that under this infusion rate of insulin (4 mU/kg/min), there was a fourfold increase in clamped serum insulin level compared with basal level, which ensured the hyperinsulinemic condition during clamp. Blood glucose (Fig. 5*B*) levels were clamped to ∼15 mg/L in HFD-fed βCASKKO and HFD-fed WT mice; during the clamp, the GIR (Fig. 5*C*) showed significant increases in the HFD-fed βCASKKO mice relative to the HFD-fed WT mice. Subsequent Western blots of liver, skeletal muscle, and epididymal adipose tissues removed immediately after completion of the clamp assays showed that although no difference was observed in AKT phosphorylation in the liver or skeletal muscle (Fig. 5*D–E*), AKT phosphorylation in adipose tissue of HFD-fed βCASKKO mice increased significantly compared with HFD-fed WT mice (Fig. 5*F*).

HFD-Fed βCASKKO Mice Showed Upregulated IRS1/PI3K/AKT Signaling Pathway in Adipose Tissue

Hematoxylin-eosin staining of insulin target tissue sections from HFD-fed mice showed lipid deposition in the liver and a significant enlargement of the sarcolemma space (Fig. 6*A–B*) and the epididymal adipocyte size (Fig. 7*A*). AKT phosphorylation in the liver and skeletal muscle showed no difference (Fig. 6*C–D*) within the HFD group, but in the adipose tissue, it was higher in HFD-fed βCASKKO mice than in HFD-fed WT mice (Fig. 7*B–C*). Further research found the phosphorylation of IRS1 serine residue, mTOR, and S6K1 was also significantly lower in adipose tissue from HFD-fed βCASKKO mice than from HFD-fed WT mice (Fig. 7*B–C*).

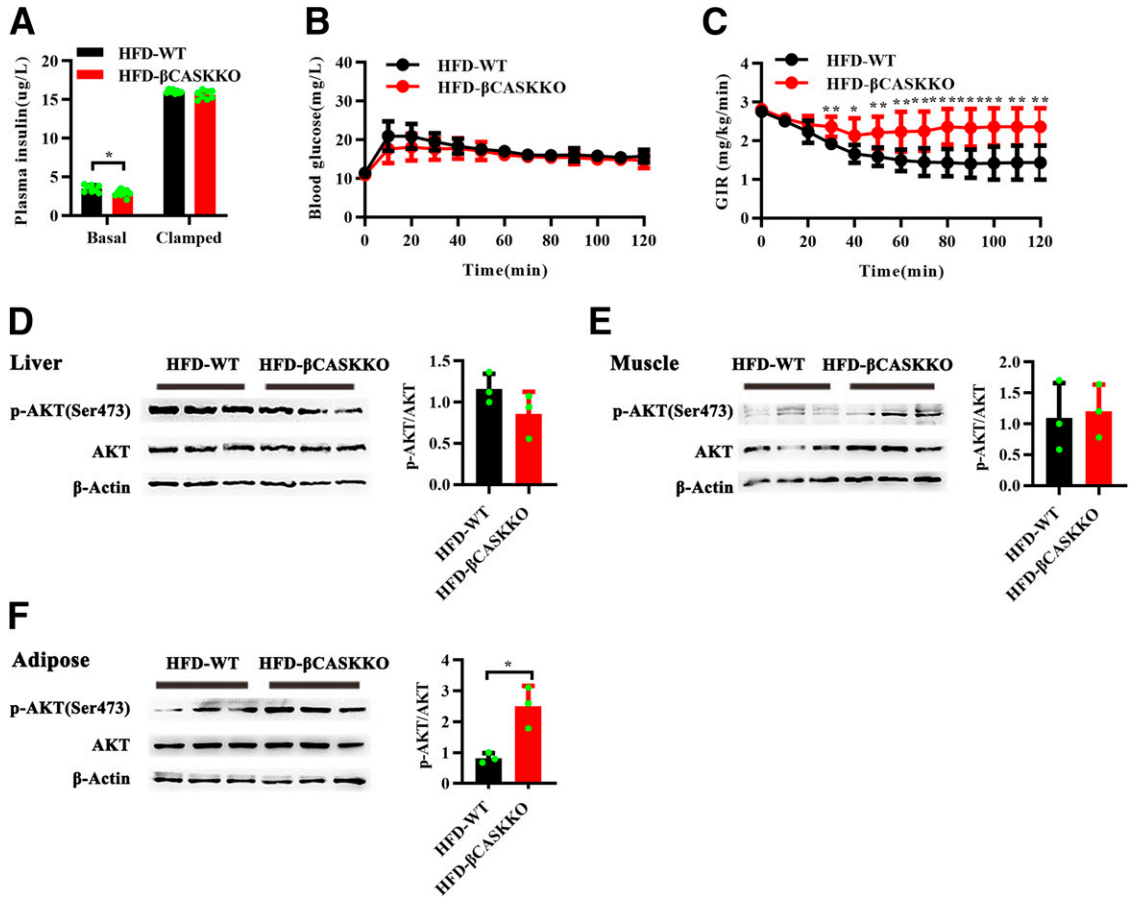

Figure 5—Hyperinsulinemic-euglycemic clamp assays were performed in HFD-mice with HFD for 16 weeks. *A*: Serum insulin levels under basal and clamped conditions ($n = 8$). *B*: Blood glucose was monitored at 10-min intervals and maintained at ~150 mg/L during the hyperinsulinemic-euglycemic clamp assay ($n = 8$). *C*: The GIR maintained the blood glucose levels during the clamp assay ($n = 8$). *D–F*: Western blot analysis of the phosphorylation level of AKT (p-AKT) in the liver (*D*), muscle tissue (*E*), and epididymal adipose tissue (*F*) of mice after the end of the clamp ($n = 3$). *$P < 0.05$, **$P < 0.01$.

DISCUSSION

In this study, we established a β-cell–specific knockout of CASK in mice and examined glucose metabolism in mice fed an ND and HFD. The findings provide the first in vivo evidence that CASK is involved in insulin secretion. Under ND feeding, with no obvious sex difference (Supplementary Fig. 4*A–F*), knockout of CASK in mouse pancreatic islet β-cells appeared to interfere with the transport or anchoring of insulin granules to the β-cell membrane, thereby inhibiting glucose-stimulated insulin secretion and increasing blood glucose after glucose challenge. Interestingly, the loss of CASK in β-cells alleviated the hyperinsulinemia caused by obesity-related diabetes. Additional results revealed that βCASKKO mice fed the HFD for 16 weeks showed attenuated insulin resistance and hyperglycemia because of improvement in the balance of the PI3K/AKT and mTOR/S6K1 signaling pathways in adipose tissue. These findings indicate βCASKKO mice had a reduced insulin secretion level, whereas after HFD feeding, improved insulin sensitivity was found in βCASKKO mice via reduction of hyperinsulinemia.

In line with our in vitro studies (9–11), the GSIS tests performed on βCASKKO mice in vivo and on isolated βCASKKO mouse islets ex vivo both revealed reduced insulin secretion in response to glucose stimulation. However, CASK deficiency in β-cells did not alter the expression of genes that regulate insulin synthesis and exocytosis, and no difference was detected in the number, morphology, or size of the insulin vesicles in βCASKKO compared with WT β-cells. Thus, these results indicate that CASK undoubtedly participates in insulin secretion, but its deletion does not cause cell death in pancreatic β-cells under physiological conditions, which also partially explains why glucose tolerance was only slightly impaired in βCASKKO mice.

It should be noted that in βCASKKO mouse islets, transmission electron microscopy imaging showed a lower number of insulin granules at or near the cell membrane. Previous reports showed that CASK recruits Mint1 through its N-terminal CaMK kinase domain in neurons and that Mint1 in turn binds to the transport protein Munc18-1, which is involved in the release of neurotransmitters

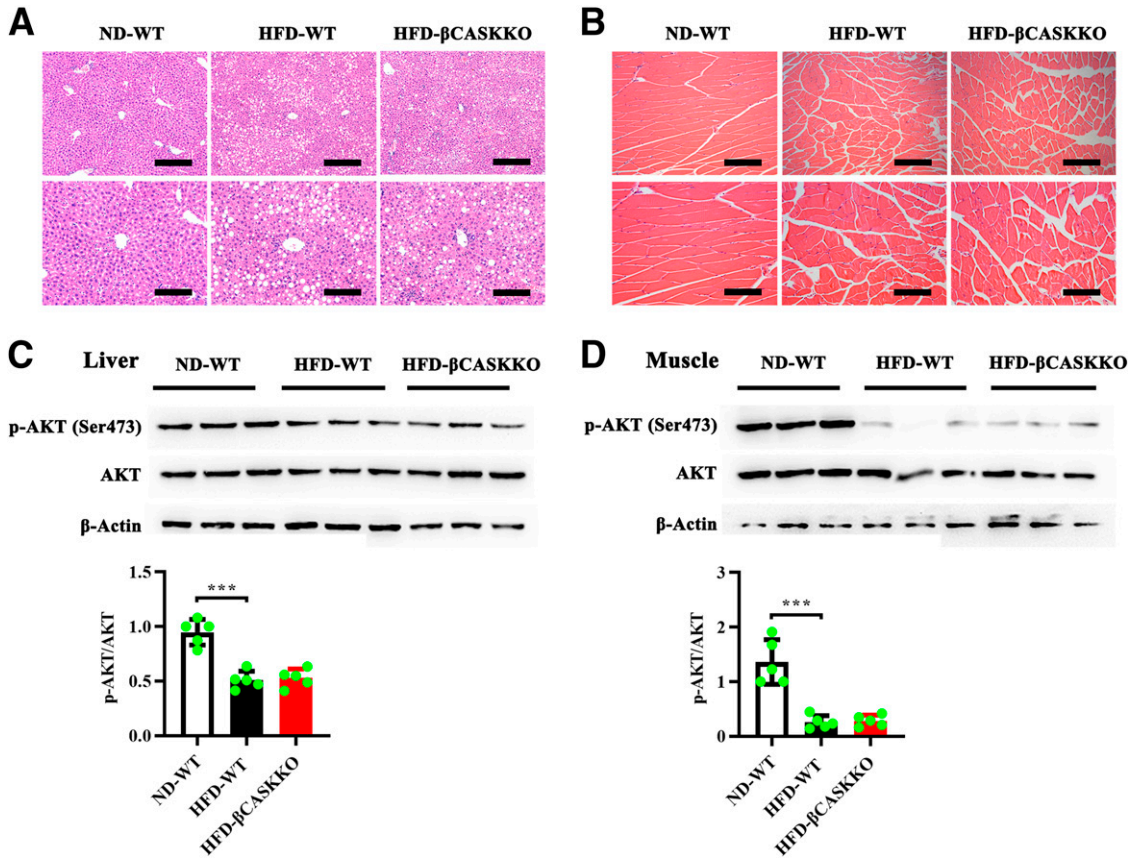

Figure 6—HFD-fed βCASKKO mice fed an HFD for 16 weeks did not show effects on insulin signaling in liver or skeletal muscle. *A–B*: Representative hematoxylin-eosin staining of the liver (*A*) and skeletal muscle (*B*) from ND-fed WT, HFD-fed WT, and HFD-fed βCASKKO mice (scale bars 200 [upper] and 100 μm [lower]). *C–D*: Representative immunoblots of the phosphorylation level of AKT (p-AKT) in the liver (*C*) and muscle tissue (*D*) of mice 15 min after insulin treatment. Protein levels were normalized to the β-actin level. The intensity of the protein bands is indicated below the respective bands ($n = 5$). ***$P < 0.001$.

(24,25). In INS-1E cells, Munc18-1 binds to the plasma membrane Q-SNARE Syntaxin1 and participates in the regulation of insulin vesicle transport (26). Recently, we (9) and Zhang et al. (27) independently reported that CASK, Mint1, and Munc18-1 interact with one another in INS-1 cells to form a triple complex to regulate insulin secretion. Therefore, considering that glucose- and potassium-initiated insulin secretion are both impaired in βCASKKO mouse islets, and exendin-4–induced insulin secretion is also attenuated in CASK knockdown INS1 cells, we speculated that CASK participates in the transport and anchoring of insulin vesicles, a common downstream step in insulin secretion, by interacting with Mint1 and Munc18, to regulate the insulin secretion in β-cells.

Moreover, we previously reported that CASK is involved in palmitate- (10), glucotoxicity- (12), or interleukin-1β–induced (13) pancreatic β-cell dysfunction. Because CASK plays a critical role in physiological insulin secretion, further evaluation of whether CASK participates in pancreatic β-cell damage during diabetes is valuable. Surprisingly, reduced hyperglycemia, glucose intolerance, insulin resistance, and hyperinsulinemia were observed in the βCASKKO mice in comparison with the WT mice after 16-week HFD treatment. Although these phenomena were not significant at 8-week exposure to HFD (Supplementary Fig. 5*A–F*), suggesting a progressive effect of βCASKKO when combined with the stress of an HFD, it seems natural to connect the reduced hyperinsulinemia in HFD-fed βCASKKO mice with CASK deletion in β-cells. Chronic exposure to hyperinsulinemia is known to be one of the important causes of metabolic abnormality in T2DM (28). Multiple studies have shown that reduced insulin secretion by GPR40 antagonism (29,30) or by murine *Ins-1* gene deletion (31), even by using streptozotocin to generate a moderate β-cell injury (32), can protect against metabolic disorders in T2DM. Similarly, we speculated that CASK deletion in β-cells would improve insulin sensitivity in HFD-fed mice through reducing the development of hyperinsulinemia. In addition, the expression of CASK was increased in HFD-fed mice compared with ND-fed mice, which is in line with the data generated

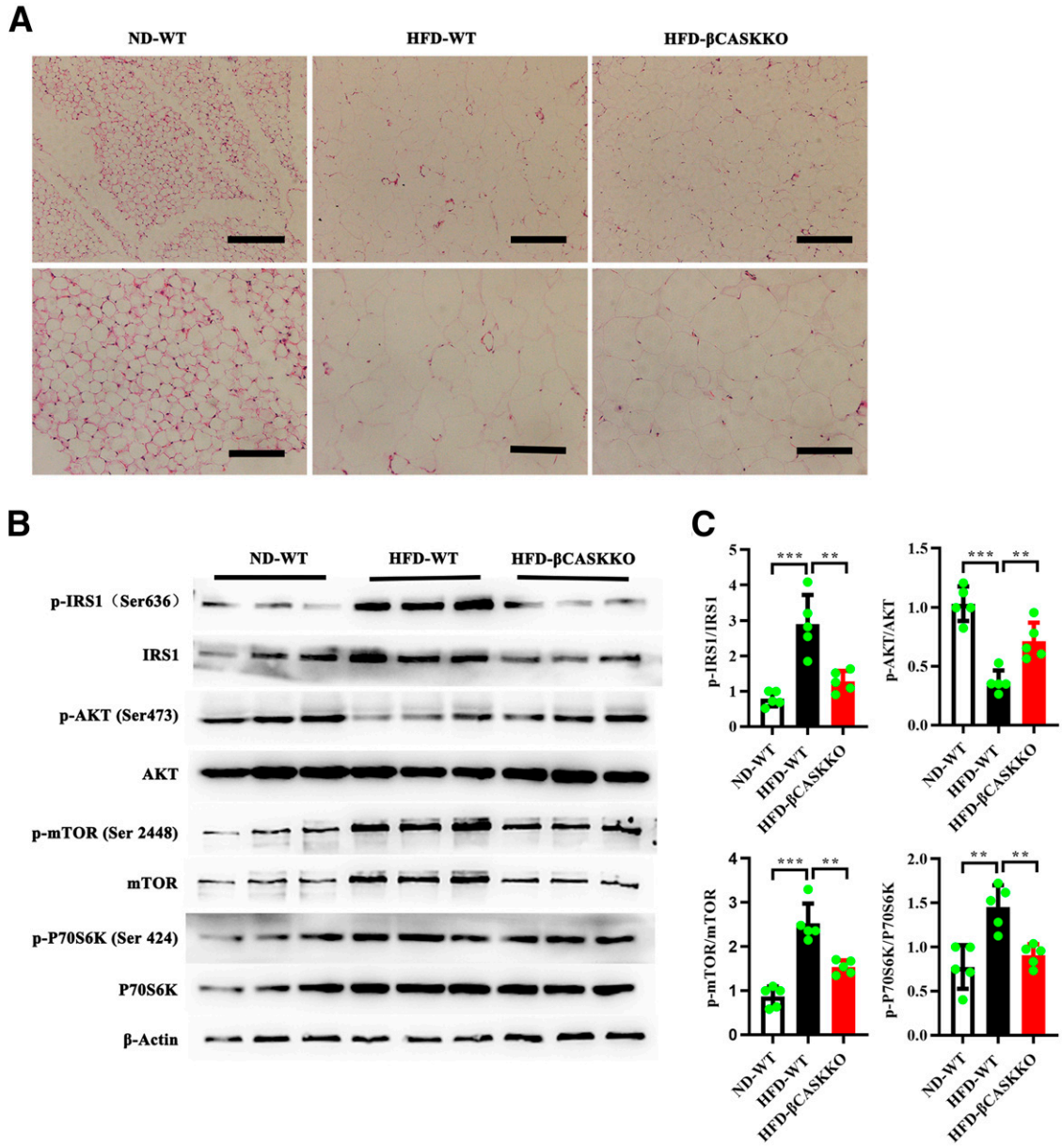

Figure 7—HFD-fed βCASKKO mice fed an HFD for 16 weeks show upregulation of the IRS1/PI3K/AKT signaling pathway in adipose tissue. *A*: Representative hematoxylin-eosin staining of adipose tissue from ND-fed WT, HFD-fed WT, and HFD-fed βCASKKO mice (scale bars 200 [upper] and 100 μm [lower]). *B–C*: Representative immunoblots (*B*) and densitometry data analysis (*C*) of IRS1, AKT, mTOR, and S6K1 phosphorylation (p) and total protein 15 min after insulin treatment of ND-fed WT, HFD-fed WT, and HFD-fed βCASKKO mice. Protein levels were normalized to those of β-actin ($n = 5$). $^{**}P < 0.01$, $^{***}P < 0.001$.

in a T2DM *db/db* mouse model (27), further proving that CASK plays some role in the development of hyperinsulinemia. Our data show that the serum insulin level in HFD-fed βCASKKO mice was reduced. Morphological staining also demonstrated that the compensatory increased β-cell mass in HFD mice was rescued by βCASKKO. Therefore, although the underlying mechanisms still require further exploration, because βCASKKO does not affect islet morphology in ND-fed mice, this present study provides convincing evidence that βCASKKO can reduce hyperinsulinemia and compensatory β-cell growth, preventing possible β-cell exhaustion during the development of T2DM.

We further assessed insulin signal transduction in the insulin target organs in HFD-fed βCASKKO mice. The IPITT and hyperinsulinemic-euglycemic clamp assays showed that HFD-fed βCASKKO mice had alleviated insulin resistance compared with HFD-fed WT mice. Notably, βCASKKO reduced the aggravation of insulin resistance mainly in the adipose tissue rather than in the liver or muscle of HFD-fed mice. One possible explanation is that during the prediabetic stage, insulin resistance first develops

in selective organs like skeletal muscle and liver because of immune-mediated inflammatory changes and excess free fatty acids when combined with the stress of an HFD, thereby causing ectopic lipid deposition in liver (33–35). Another explanation could be that in this prediabetic stage, impaired glucose uptake in muscle causes a compensatory increase of insulin sensitivity in adipose to accept shunted glucose. However, with the development of insulin resistance and hyperinsulinemia, decompensation occurs in adipose tissue, causing suppressed lipolysis and increased inflammation. The increased circulating FFAs further exacerbate global insulin resistance (36,37). Thus, this compensation-decompensation mechanism of insulin sensitivity in adipose suggests that adipocytes are one of the most insulin-sensitive cell types (37); we speculate that the reduced hyperinsulinemia by βCASKKO mainly benefits the insulin sensitivity in adipose tissue in our study, but this was not enough to reduce insulin resistance in muscle or liver because of the unchanged fat mass and circulating lipid level. Although the effect of βCASKKO on insulin signals in different organs when combined with the stress of an HFD requires further investigation, this result still suggests that the improved glucose homeostasis and insulin sensitivity in HFD-fed βCASKKO mice occurred through reduced hyperinsulinemia by specific deletion of CASK in β-cells.

In conclusion, the current study indicates that knockout of the *Cask* gene in β-cells has a diverse effect on glucose homeostasis, reducing insulin secretion in ND-fed mice but improving insulin sensitivity in HFD-fed mice via reduction in hyperinsulinemia. These findings provide novel evidence to support investigation of CASK as a therapeutic target for insulin secretion and treatment of T2DM.

Funding. This study was supported by research grants 81570734 (Y.W.), 81830024 (X.H.), and 81603169 (P.S.) from the National Natural Science Foundation of China and the open fund of State Key Laboratory of Pharmaceutical Biotechnology from Nanjing University of China (KF-GN-201704).

Duality of Interest. No potential conflicts of interest relative to this article were reported.

Author Contributions. X.L. and P.S. wrote the manuscript. X.L., P.S., Q.Y., J.X., T.X., K.Z., and X.C. performed the experiments. X.L., P.S., T.X., K.Z., and L.Y. analyzed the data. Y.W. conceived and designed the study and participated in editing and reviewing the manuscript. L.Y. provided technical guidance, analyzed data, and revised the manuscript. X.H. was responsible for the study design, technical guidance, and revision of the manuscript. Y.W., L.Y., and X.H. are the guarantors of this work and, as such, had full access to all the data in the study and take responsibility for the integrity of the data and the accuracy of the data analysis.

References

1. Zhuang Y, Xing C, Cao H, et al. Insulin resistance and metabonomics analysis of fatty liver haemorrhagic syndrome in laying hens induced by a high-energy low-protein diet. Sci Rep 2019;9:10141

2. Hou JC, Min L, Pessin JE. Insulin granule biogenesis, trafficking and exocytosis. Vitam Horm 2009;80:473–506

3. Kojta I, Chacińska M, Błachnio-Zabielska A. Obesity, bioactive lipids, and adipose tissue inflammation in insulin resistance. Nutrients 2020;12:1305

4. Petersen MC, Shulman GI. Mechanisms of insulin action and insulin resistance. Physiol Rev 2018;98:2133–2223

5. Roth Flach RJ, Danai LV, DiStefano MT, et al. Protein kinase mitogen-activated protein kinase kinase kinase kinase 4 (MAP4K4) promotes obesity-induced hyperinsulinemia. J Biol Chem 2016;291:16221–16230

6. Suckow AT, Comoletti D, Waldrop MA, et al. Expression of neurexin, neuroligin, and their cytoplasmic binding partners in the pancreatic beta-cells and the involvement of neuroligin in insulin secretion. Endocrinology 2008;149:6006–6017

7. Hsueh YP. The role of the MAGUK protein CASK in neural development and synaptic function. Curr Med Chem 2006;13:1915–1927

8. Hsueh YP. Calcium/calmodulin-dependent serine protein kinase and mental retardation. Ann Neurol 2009;66:438–443

9. Zhang K, Wang T, Liu X, et al. CASK, APBA1, and STXBP1 collaborate during insulin secretion. Mol Cell Endocrinol 2021;520:111076

10. Wang Y, Lin H, Hao N, et al. Forkhead box O1 mediates defects in palmitate-induced insulin granule exocytosis by downregulation of calcium/calmodulin-dependent serine protein kinase expression in INS-1 cells. Diabetologia 2015;58:1272–1281

11. Zhu ZQ, Wang D, Xiang D, Yuan YX, Wang Y. Calcium/calmodulin-dependent serine protein kinase is involved in exendin-4-induced insulin secretion in INS-1 cells. Metabolism 2014;63:120–126

12. Wang Y, Hao N, Lin H, Wang T, Xie J, Yuan Y. Down-regulation of CASK in glucotoxicity-induced insulin dysfunction in pancreatic β cells. Acta Biochim Biophys Sin (Shanghai) 2018;50:281–287

13. Wang TY, Liu XJ, Xie JY, Yuan QZ, Wang Y. Cask methylation involved in the injury of insulin secretion function caused by interleukin1-β. J Cell Mol Med 2020;24:14247–14256

14. Atasoy D, Schoch S, Ho A, et al. Deletion of CASK in mice is lethal and impairs synaptic function. Proc Natl Acad Sci USA 2007;104:2525–2530

15. Srivastava S, McMillan R, Willis J, et al. X-linked intellectual disability gene CASK regulates postnatal brain growth in a non-cell autonomous manner. Acta Neuropathol Commun 2016;4:30

16. Tamarina NA, Roe MW, Philipson L. Characterization of mice expressing Ins1 gene promoter driven CreERT recombinase for conditional gene deletion in pancreatic β-cells. Islets 2014;6:e27685

17. Carboneau BA, Le TD, Dunn JC, Gannon M. Unexpected effects of the MIP-CreER transgene and tamoxifen on β-cell growth in C57BI6/J male mice. Physiol Rep 2016;4:e12863

18. Zhu Y, You W, Wang H, et al. MicroRNA-24/MODY gene regulatory pathway mediates pancreatic β-cell dysfunction. Diabetes 2013;62:3194–3206

19. Xiong J, Sun P, Wang Y, et al. Heterozygous deletion of Seipin in islet beta cells of male mice has an impact on insulin synthesis and secretion through reduced PPARγ expression. Diabetologia 2020;63:338–350

20. Heikkinen S, Argmann CA, Champy MF, Auwerx J. Evaluation of glucose homeostasis. Curr Protoc Mol Biol 2007;Chapter 29:Unit 29B.3

21. Faleck DM, Ali K, Roat R, et al. Adipose differentiation-related protein regulates lipids and insulin in pancreatic islets. Am J Physiol Endocrinol Metab 2010;299:E249–E257

22. Li K, Qiu C, Sun P, et al. Ets1-mediated acetylation of FoxO1 is critical for gluconeogenesis regulation during feed-fast cycles. Cell Rep 2019;26:2998–3010.e5

23. Jiang S, Shen D, Jia WJ, et al. GGPPS-mediated Rab27A geranylgeranylation regulates β cell dysfunction during type 2 diabetes development by affecting insulin granule docked pool formation. J Pathol 2016;238:109–119

24. Hata Y, Butz S, Südhof TC. CASK: a novel dlg/PSD95 homolog with an N-terminal calmodulin-dependent protein kinase domain identified by interaction with neurexins. J Neurosci 1996;16:2488–2494

25. Maximov A, Bezprozvanny I. Synaptic targeting of N-type calcium channels in hippocampal neurons. J Neurosci 2002;22:6939–6952

26. Tomas A, Meda P, Regazzi R, Pessin JE, Halban PA. Munc 18-1 and granuphilin collaborate during insulin granule exocytosis. Traffic 2008;9:813–832

27. Zhang Z, Li W, Yang G, et al. CASK modulates the assembly and function of the Mint1/Munc18-1 complex to regulate insulin secretion. Cell Discov 2020;6:92
28. Gao Z, Wang Z, Zhu H, et al. Hyperinsulinemia contributes to impaired-glucose-tolerance-induced renal injury *via* mir-7977/SIRT3 signaling. Ther Adv Chronic Dis 8 May 2020 [Epub ahead of print]. doi:10.1177/2040622320916008
29. Steneberg P, Rubins N, Bartoov-Shifman R, Walker MD, Edlund H. The FFA receptor GPR40 links hyperinsulinemia, hepatic steatosis, and impaired glucose homeostasis in mouse. Cell Metab 2005;1:245–258
30. Sabrautzki S, Kaiser G, Przemeck GKH, et al. Point mutation of Ffar1 abrogates fatty acid-dependent insulin secretion, but protects against HFD-induced glucose intolerance. Mol Metab 2017;6:1304–1312
31. Szabat M, Page MM, Panzhinskiy E, et al. Reduced insulin production relieves endoplasmic reticulum stress and induces β cell proliferation. Cell Metab 2016;23:179–193
32. Pedersen DJ, Guilherme A, Danai LV, et al. A major role of insulin in promoting obesity-associated adipose tissue inflammation. Mol Metab 2015;4:507–518
33. Perseghin G, Petersen K, Shulman GI. Cellular mechanism of insulin resistance: potential links with inflammation. Int J Obes Relat Metab Disord 2003;27:(Suppl. 3):S6–S11
34. Zhang X, Shao H, Zheng X. Amino acids at the intersection of nutrition and insulin sensitivity. Drug Discov Today 2019;24:1038–1043
35. Stahl EP, Dhindsa DS, Lee SK, Sandesara PB, Chalasani NP, Sperling LS. Nonalcoholic fatty liver disease and the heart: JACC state-of-the-art review. J Am Coll Cardiol 2019;73:948–963
36. Kim JK, Michael MD, Previs SF, et al. Redistribution of substrates to adipose tissue promotes obesity in mice with selective insulin resistance in muscle. J Clin Invest 2000;105:1791–1797
37. Kahn BB, Flier JS. Obesity and insulin resistance. J Clin Invest 2000;106:473–481